SPI SCIENCE VALIDATION REPORT

Action IUG/01/04

Prepared by:	Signature:
Elisabeth JOURDAIN **Chris SHRADER** **Jean-Pierre ROQUES**	
Accepted by:	Signature:
Jean-Pierre ROQUES	
Approved and Application authorised by:	

Number of pages: 28

Secretariat of origin: CESR - Pascale Ramon

Host system: PC Pentium III 600

Host software:

Word Processing	Drawings
Word 2000	/

C.E.S.R.	EXTERNAL DISTRIBUTION
	INTEGRAL User Group INTEGRAL Science Data Centre

DOCUMENT CHANGE RECORD

Edition	Revision	Date	Modified pages	Observations
1	0	05/08/05	/	Creation

- TABLE OF CONTENTS -

I - INTRODUCTION

The aim of this document is to provide validation information on central high level tools delivered by the SPI team to the ISDC. The validation of the entire SPI data reduction system at the ISDC is out of the scope of this document as several tools and scripts have been developed under the ISDC responsibility.
This document will thus focus on:

- Validation of the SPI calibration files: Imaging response IRF and energy redistribution response RMF.
- Validation of SPIROS: SPI iterative Removal of Sources. SPIROS is the key point of SPI scientific data analysis that provides images, spectra and light curves adapted to various situations.
- Validation of XSPEC12: This evolution of XSPEC is able to handle the complete SPI response in presence of the dithering. This is thus an alternative to SPIROS for the spectral extraction.

This validation will be done using real scientific data, focusing into the intrinsic performances of the tools. Thus this validation has not always been realised in the framework of the ISDC system in order to validate the tools themselves. We can't be exhaustive: other validation documents exist and will be cited as appropriate.

II -VALIDATION OF SPI CALIBRATION FILES OSA5.0

The calibration files cover 3 epochs of SPI camera life:

- Switch-on to Rev 139 where all detector chains were alive
- Revolutions 141 to 214
- From revolution 215

Revolution 140 corresponds to the failure of GeD 2, while GeD17 failed between Rev 214 and 215.
The complete SPI calibration process has been initiated well before the launch and relies on monte-carlo simulations, a complete mass model of both SPI and the spacecraft and on calibrations with radioactive sources done at various stages of SPI development. In particular a long calibration campaign has been conducted at Bruyeres-Le-Chatel. A lot of details of this validation process can be found in:
Sizun, P., et al, 2004, proc. Fifth INTEGRAL Workshop, SP-552
Skinner, G., & Connell, P., 2003, A&A, 411, L123
Sturner, S., et al., 2003, A&A, 411, L81
Attie, D., et al., 2003, A&A, 411, L71
Roques J.P.et al, 2003, A&A, 411, L91

Here we will focus on the validations done in-flight using the Crab Nebula as a reference source. The following points will be addressed:

- Spectral reconstruction and Crab spectral parameters:

  - Comparison with previous results
  - Fit parameters stability for different epoches.
- Flux stability with the source position in the field of view
- Flux stability with time.

.

The results presented here have been obtained "outside" the ISDC system: data processing, spectral extraction and spectra model fitting have been performed within our S-GSE (Science Ground Support Equipment) system. The reasons are the following:

- The "standard" ISDC spectral extraction scheme is based on SPIROS that doesn't use the energy redistribution matrix.
- Our goal is here to check the matrices independently of the complete analysis system.

Data used:

No revolution	Date (beg-end) Yy/mm/dd	Useful Duration	comments	Particular pointing Pattern (see Fig. II-1)
000045	03/02/25-27	161 176 s	19 detectors	Off axis 0°-5°-7°-10°
000170	04/03/05-06	125 515 s	18 detectors	Off axis up to 14°. See fig1
000239	04/09/27-30	166 210 s	17 detectors	½ circle between 2° and 4°
000300	05/03/29-31	104 970 s	17 detectors	10° circle in the 2nd part

Table 1: main information about the data used in this work

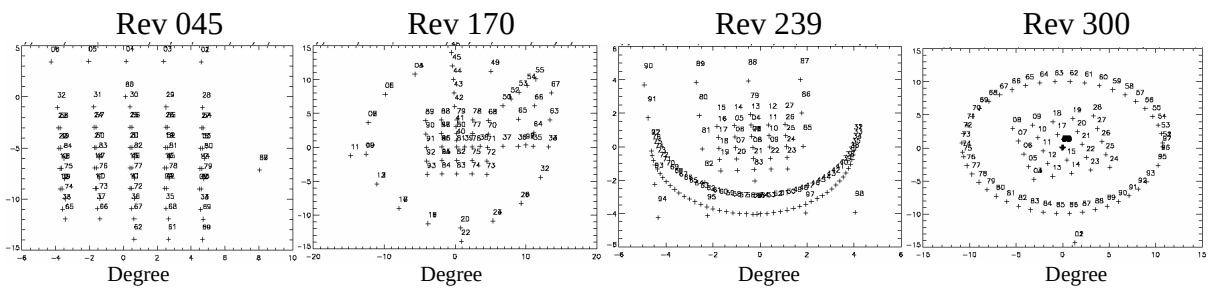

Figure II-1: Dithering patterns for the revolutions used in this work (the Crab position is 0,0)

II-A : Crab Spectra reconstruction

3% systematic error has been added to the statistical errors.

<u>II-A-1: The Matrices validation</u>

The Crab spectrum has been built for 3 revolutions (045, 170 and 239) with respectively 19, 18 and 17 detectors. We fit them with a broken power law model between 23 and 8000 keV . To allow simple comparison, we have fixed the Break energy at 90 keV.
The best fit parameters are presented in table 1 and the spectra in Fig II-2.

Rev #	Index 1	Ebreak (keV) fixed	Index 2	Norme @ 100 keV (ph cm-2 s-1)
45	2.14 +/-.8 10^{-2}	90.0	2.29 +/- 110^{-2}	6.3 E-04
170	2.14 +/-.8 10^{-2}	90.0	2.31 +/- 1.4 10^{-2}	6.04 E-04
239	2.14 +/-.8 10^{-2}	90.0	2.35 +/- 1-1.4 10^{-2}	6.00 E-04

Table 1: best fit parameters with a broken powerlaw
These parameters are in perfect agreement with values obtained by other experiments in the same energy range (see Sizun et al., (2004) for a brief review)

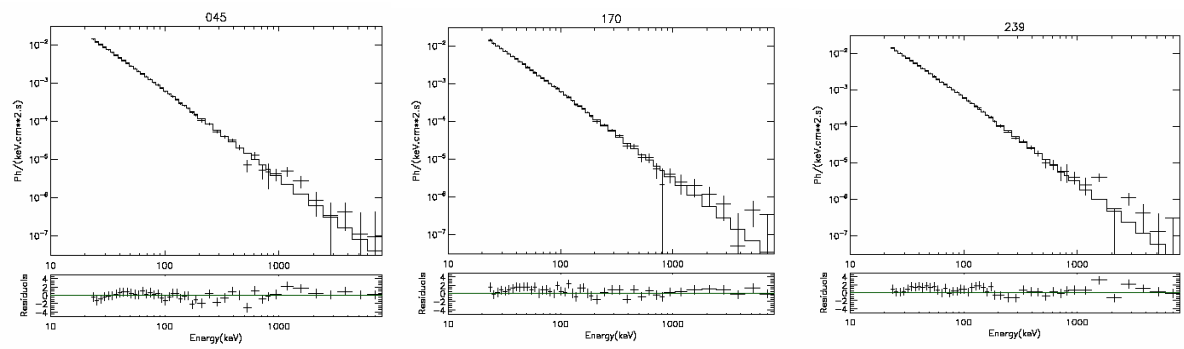

Fig II-2: Crab spectra with the broken powerlaw model

Systematics appear around 1.5 MeV due to a non corrected electronic feature

II-A-2: Low energy efficiency overestimation

A clear deviation appears below ~ 23 keV in all the Crab spectra (see fig II-3), as the instrumental response in not easy to determine in this domain. We thus recommend to use SPI only above this energy for strong sources.

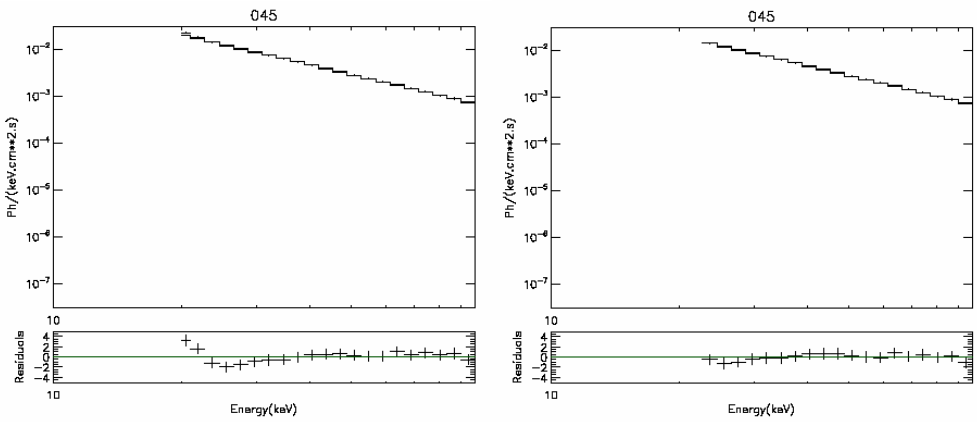

Fig II-3: The low energy part of SPI spectra with and without the first channels

II-A-3: Off-axis versus on-axis response

Using the revolution 300 (see fig II-1), we have built a spectrum "on-axis" (0°< Θ < 5.7°) and "off-axis" (Θ ~ 10°). The fig II-4 shows the ratio between both spectra, which is very close to 1 at least up to 200 keV where the statistics becomes too low to conclude.

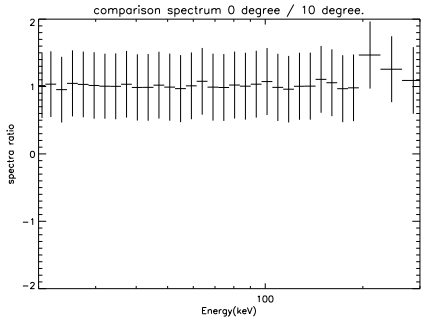

Fig II-4 : ratio between on-axis and off-axis spectra.

II-B: Flux versus off-axis angle Θ

The Crab flux is presented versus the angular distance between the source direction and SPI axis for the 3 same revolutions (045, 170 and 239), in the 25-45 keV and 40-80 keV bands (fig II-5).

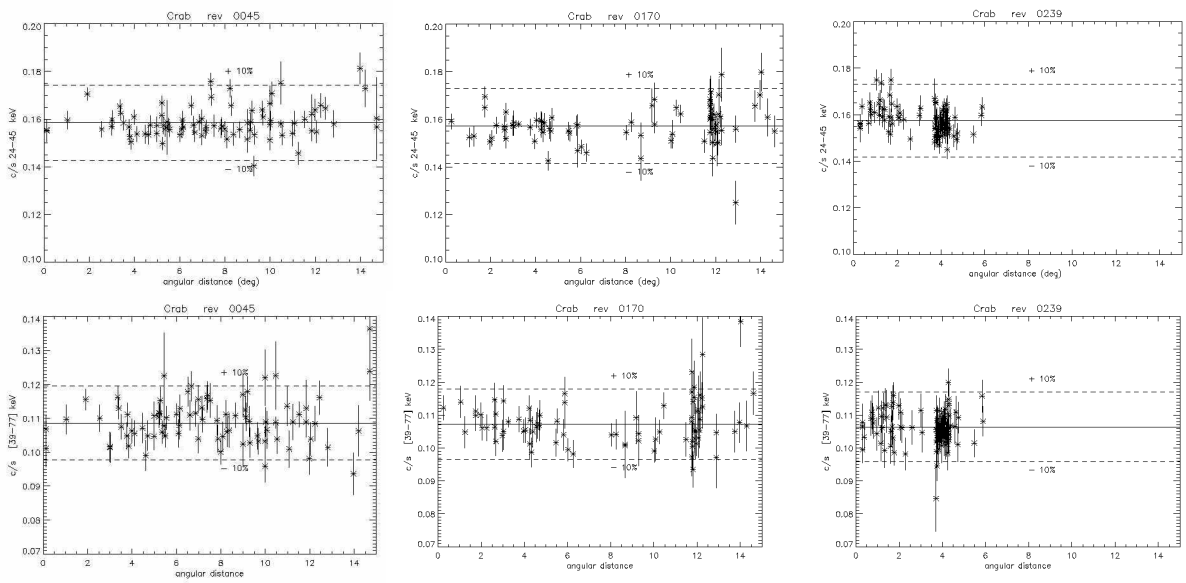

Fig II-5: Crab flux extracted (1 scw timescale) versus the off-axis angle.

The flux remains stable within +- 10 %, except in some cases with large off-angles (> 12°), whatever the detector plan status. This illustrates as well the instrument stability with time.

II-C: Conclusions

The response matrices give results in agreement with what we expect in a well known stable source.

They represent thus perfectly the instrument which appears moreover very stable with time, in all configurations (19-17 detectors).
The only restrictions concern the domain below 23 keV and some off-axis angle values greater than 12 ° ie a very small amount of data.

III - SPIROS VALIDATION.

The SPIROS version delivered for OSA5 is V9.2
SPIROS heavily relies on the IRF part of the calibration files, thus the results presented here rely both on SPIROS and the IRF calibration files (this was also a reason to validate the IRF with independent tools).
SPIROS can be used in several configurations; we will discuss:

- Imaging mode: sources search and/or model fitting (use of an input catalogue).
- Timing mode (light curve extraction)
- Spectral mode (spectrum reconstruction)
- Background handling modes.

SPIROS principles and modes are detailed in SPIROS user manual (P. Connell, http://isdc.unige.ch/index.cgi?Support+spi and click on document tree). The basics description can be found in Skinner & Connell (2003) while SPIROS performance has been studied in Dubath et al (2005).
SPIROS is delivered together with a set of example and test files for validation.
Here we will concentrate on a few examples which validate SPIROS basic modes on real data.

III - A: Imaging mode: Crab observation revolution 44

SPIROS source search is enabled when the number of sources to be searched (nofsources) in spiros.par is greater than 0.
Source flux model fitting is enabled when an input catalogue is specified. This catalogue contains the positions of the sources to be considered.
These two ways of flux extraction/image generation can be used simultaneously (for more details see SPIROS documentation).

The background handling mode used here is mode 3 (background_method parameter in spiros.par). This mode needs a reference empty field observation which has been constructed with revolution 72.

TEST N°1:

Input data: Crab observation in revolution 44.
Energy band: 25-45 keV
Nofsources: 5
Input catalogue: none

The logarithmic scale shows the residuals distribution in the image.
The Crab position found is less that 1 arc minute away from the true position.
The Crab is detected at 495 σ. The next excess is detected at 7.2 σ. The systematic errors due to the IRF are thus < 2%.

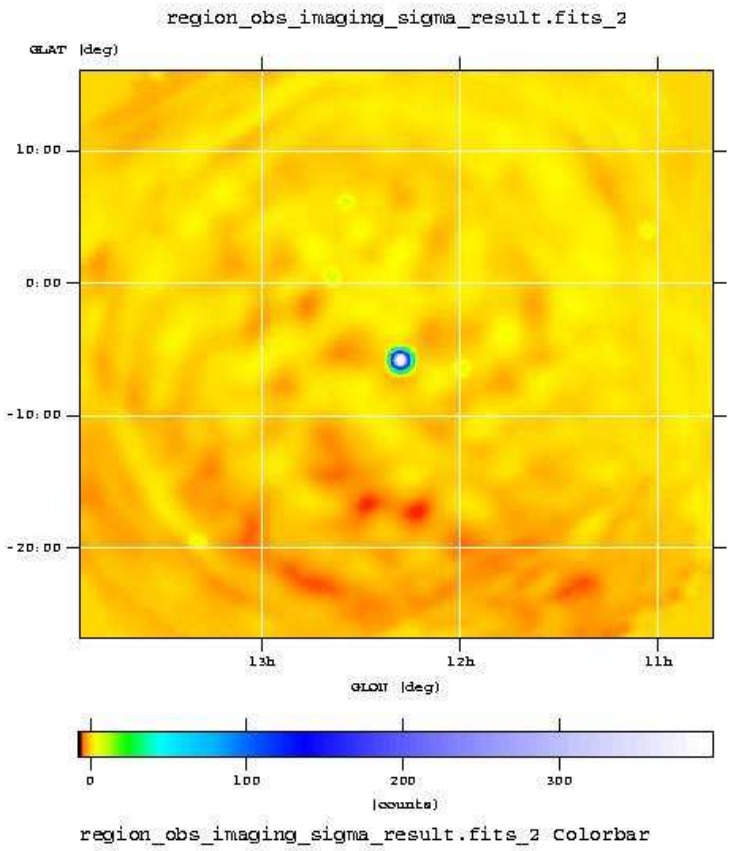

TEST N°2

Input data: Crab observation in revolution 44.
Energy band: 25-45 keV
Nofsources: 0
Input catalogue: Crab position

The image produced is shown in the figure.
The source significance is 516 σ.
The residuals are below 10 σ, thus again the systematics are < 2 %

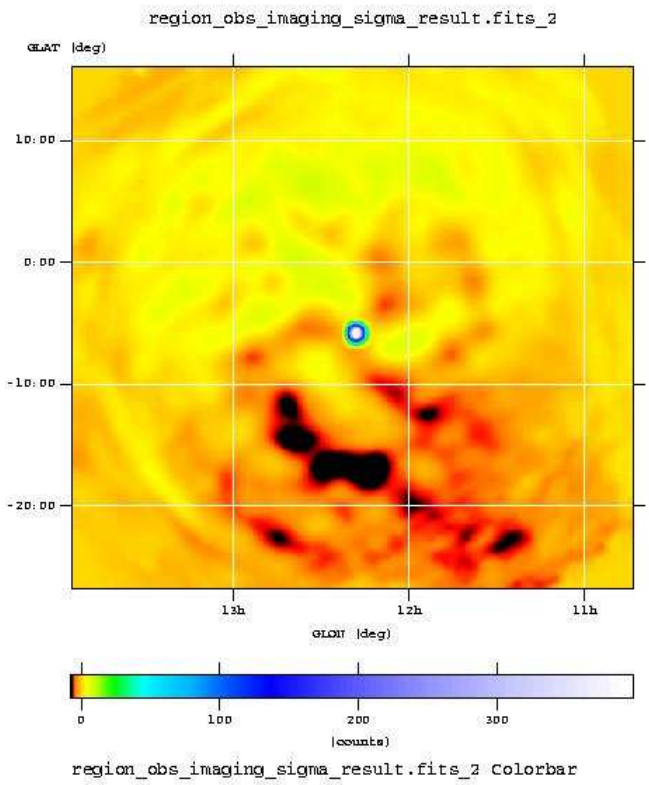

TEST N°3

Input data: Crab observation in revolution 44.
Energy band: 25-45 keV
Nofsources: 5
Input catalogue: Crab position

The image produced is shown in the figure.
The source significance is 492 σ.
The next excess is detected at 7.7 σ, again the systematics are lower than 2%

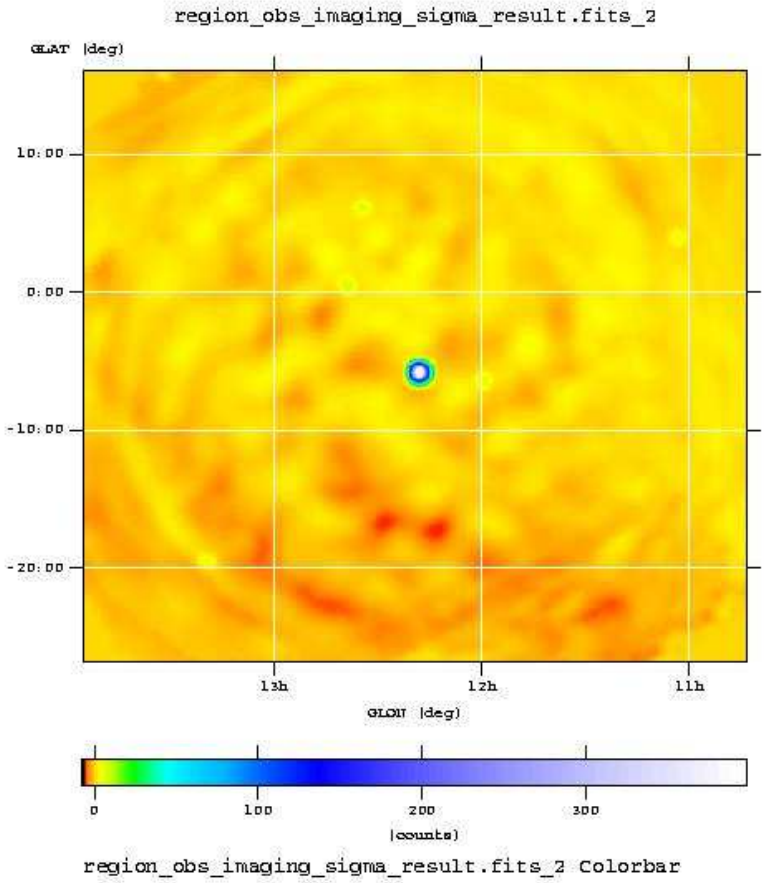

III-B: Imaging mode: GX339-4 field in revolution 166

Background mode used: 3, with empty field from rev 158
Energy band: 27-43 keV
Input catalogue: 7 sources: 4U1700-377, H1705-440, 4U1630-47, GX354-0, GX340+0, H1636-536/V*V801Ara, OAO1657-415.
Nofsources: 5

The SPIROS image exhibits 4 sources in addition to the input catalogue, identified respectively with IGR16316-4028, GX339-4, XTEJ1710-280, SAXJ1712.6-3739.

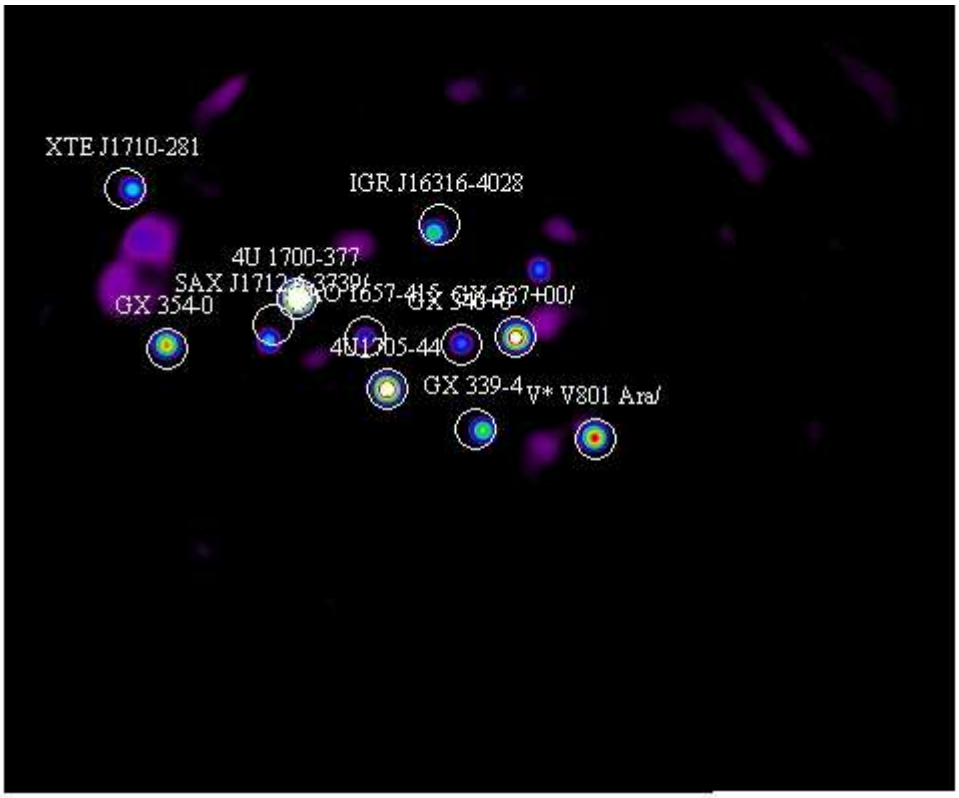

This is a quite complex case because, at least one bright flaring source, 4U1700-377, is in the partially coded field of view (thus having a highly variable coding factor). As SPIROS, in this mode, looks for a sky model with constant source fluxes, some artefacts appear in the image. In practice, SPIROS produces a quite good image, but the χ^2 is high, the imaging mode being not adapted to this configuration as it assumes constant sources.
The timing mode suits this case, but doesn't produce images!

III-C: Timing mode: GX339-4 observation in revolution 166.

In timing mode SPIROS extracts the sources and background fluxes, on various timescales. The timescales can be different for each of the specified sources (and background), thus the user can adjust the number of free parameters for a given analysis. SPIROS works in model fitting mode with one free parameter per time bin for all the defined sources and background. Details are given in SPIROS documentation.

During this GX339-4 field observation, several sources are significantly detected in the FOV, In particular 4U1700-377 which exhibits a strong erratic flaring activity.

The background handling mode has been set to 3 (constant).
The sky model input for SPIROS consists of 11 sources allowed to vary on different timescales:

- 4U1700-377: 0.0417 day (1 H, ~ 1 scw)
- GX337-0 : 0.1259 day (3 H, ~ 3-4 scws)
- GX340+0 : 0.1259 day
- GX339-4, H1705-440, GX354-0, IGR16316-4028, OAO1657-415, SAXJ1712.6, XTEJ1710-281, H1636-536 : constant.

The convergence achieved by SPIROS with this sky model is good, with a reduced χ^2 of 2

The light curves of 4U1700-377 and GX337-0 produced in the 25-45 keV energy band are shown hereafter.

.

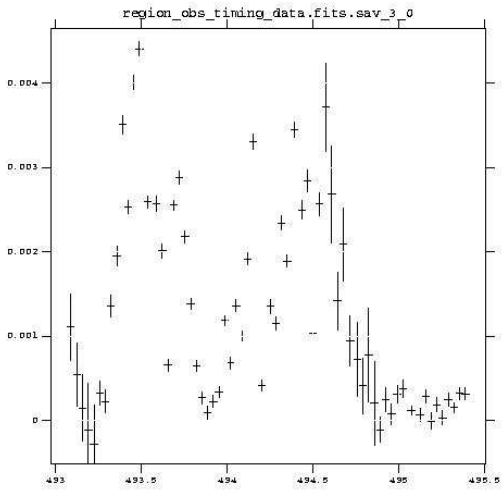

4U1700-377

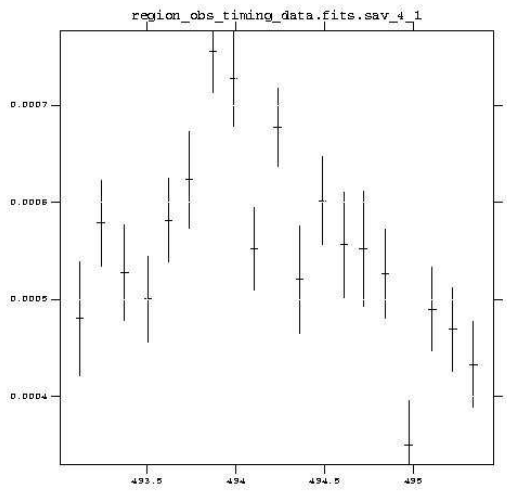

GX337-0

III-D: Spectral mode

In this mode, SPIROS produces source spectra compatible with XSPEC inputs.
We have analysed Crab data of revolution 102, with background mode parameter 2 and 5 (see below) . The spectrum has been fitted by a power law and is shown in the next figure. The best fit parameters are very close in both cases with a photon index = 2.14, and a 100 keV flux = 6.14 10-4 ph/cm2/s/keV.
These values are moreover in agreement with the results presented in Section II.

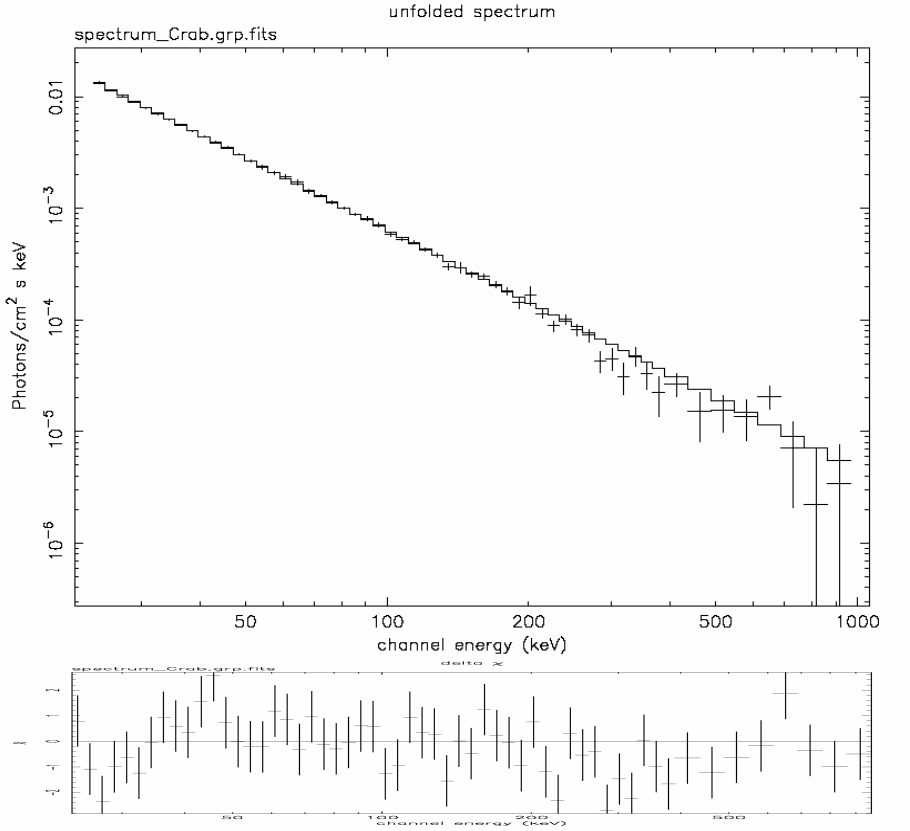

Crab spectrum, Rev 102

III-E: Background modes

SPIROS can handle the background in various ways:

- Mode 1: all detectors have the same background, USELESS
- Mode 2: a background is determined for each detector
- Mode 3: The detector ratios are fixed, SPIROS determine the normalisation
- Mode 4: Same as mode 3, but SPIROS uses the pseudo-detectors (multiple events) NOT TESTED
- Mode 5: Mean Count Modulation, automatic determination of the background

Mode 1 is useless as it is known that the background is different for each detector.

SPIROS has been tested on Cygnus X-1 observation: revolutions 20 and 159. The results are in the next table. Except for mode 1 which should NOT be used, the results are consistent, as expected when the background is stable. Significances are lower in mode 2 than in mode 3 because we have 18 more degrees of freedom.

			CYGNUS X-1		CYGNUS X-3		EXO 2030+375		
REV	BANDE D'ENERGIE	MODE BDF	INTENSITE (mCrab)	SIGNIFICATIVITE (σ)	INTENSITE (mCrab)	SIGNIFICATIVITE (σ)	INTENSITE (mCrab)	SIGNIFICATIVITE (σ)	χ^2/ν
159	20-25 keV	1	1364,4	52,8	555,1	50,9			1,89
		2	1314,8	42,8	414,9	25,2			1,54
		3	1301,6	49,5	414,5	27,3			1,6
		5	1294,9	47,9	422,3	27,3			1,46
	25-45 keV	1	857,6	171,2	241,6	109,6			5,32
		2	825	138	174,2	52,7			3,68
		3	831,1	163,4	176,1	57			3,78
		5	829,6	159,7	178,9	56,8			3,16
	200-400 keV	1	856,6	19,8					1,24
		2	456,3	6,2					1
		3	451,6	8,2					1,01
		5	429,4	7,7					0,95
20	20-25 keV	1	835	102,7	90,1	9,3	46	4,7	1,24
		2	895,5	94	149,5	12,4	111	9,2	1,08
		3	895,8	95	168,1	14,7	122,5	10,6	1,13
		5	897,3	94,3	166	13,4	124,4	10	0,99
	25-45 keV	1	645	361,5	73,7	37,6	61	30,2	2,59
		2	643,7	313,5	69,4	27,8	57,2	22,8	2,56
		3	644,1	316,7	72,6	31	59,9	25,1	2,59
		5	645	316,9	80,8	32,1	62,3	24,2	1,73
	200-400 keV	1	695,3	39,3					4,17
		2	666,2	23,4					1,66
		3	672,4	23,8					1,69
		5	679	23,8					1,02

IV - XSPEC 12: CAPABILITIES FOR CODED-MASK SPECTRAL ANALYSIS

IV-A: CODED MASK SPECTRAL ANALYSIS

The XSPEC software package, which utilizes the "forward-folding" method of spectral analysis, has been in wide use throughout high-energy astrophysics for more than a decade. This is due to several factors: it includes a rich database of physical models, it incorporates flexible multi-mission capabilities, and it is rigorously configuration managed. However, the instruments onboard INTEGRAL, or others utilizing the coded-mask imaging technique, pose new challenges to the forward-folding method. This is a result of wide fields of view combined with the inherent inability of coded aperture experiments to directionally tag photons leading to source confusion, the complex and often predominant instrumental backgrounds, and the highly-direction-sensitive instrument response.

On the other hand, hard X-ray and gamma-ray instruments have spectral response matrices characterized by substantial off-diagonal elements. As such, the optimum use of such an instrument as a spectrometer requires a rigorous forward-folding analysis.

Here we describe some functionality that has been incorporated in to the version 12 release of the “XSPEC” software package to address these issues. In particular, we discuss the implementation of INTEGRAL/SPI-specific capabilities to (*i*) fit multiple sources with distinct physical models & responses within a single FoV, (*ii*) simultaneously solve for the instrumental background and (*iii*) manipulate large numbers of response matrices in a memory-efficient manner within the context of relatively simple command line syntaxes.

IV-B: APPLICATION TO INTEGRAL/SPI

The problem, as it specifically pertains to INTEGRAL/SPI can be summarized as follows. There are typically multiple sources within the large (16° FC) FoV. Each source is viewed by ~19 detectors, and some ~ 10's to 100's of raster points comprise a typical observation. This leads to the requirement for ~100's to 1000's of individual spectra and response matrices to be utilized in the solution. As noted, photons are not directionally tagged, so there is always potential source confusion. Additionally, the instrumental background is complex, and can vary over time or detector element or both. Furthermore, the SPI response matrices have large off-diagonal terms, and are highly directional (Sturner et al. 2003; Attie et al 2003; Sizun et al. 2004). These characteristics argue for a rigorous forward folding approach to the SPI spectral de-convolution problem.

IV-B-1 Mathematical Formulation

We now consider the SPI spectral de-convolution problem in detail. First, we assume an image reconstruction has been performed or a reliable source catalog exists covering the FoV, *i.e.* the *positions of the sources to be modeled are known*. Next, we consider a data space of the form: C=C(d, p, I); where the indices are d = detector id, p = raster point, and I = channel number. For n sources in the FoV, some subset may be visible to a given detector for a given

$$\chi^2 = \sum_p \sum_d \sum_I \left\{ \frac{\left[D_{d,p}(I) - \sum_j \sum_E R^j_{d,p}(I,E) \alpha M_j\left(E;\mathbf{x}_s\right) - B_{d,p}(I;\mathbf{x}_b) \right]}{\sigma(I)_{d,p}} \right\}^2$$

raster point, with varying degrees of shadowing. This information is contained in the response matrices. Enumerating over detectors and raster points leads to a $\partial\chi^2 / \partial \mathrm{I}$ minimization problem to perform.

In addition to the aforementioned complexities, a few additional issues pertain to SPI. Photons can undergo partial energy loss in one detector, or combinations of detectors, or in passive materials within the telescope assembly. Furthermore, in addition to the actual 19 detectors, multiple-detector events, a separate subset of events are those which trigger the pulse-shape discrimination (PSD) logic. Collectively, these different event classes necessitate consideration of ~100 virtual or "pseudo" detectors (Diehl et al 2003; Sturner et al 2003). In practice, the PSD data have not proven to be beneficial to most analyses. Nonetheless, it is clear that a large data-space will inevitably be entailed in SPI analysis.

IV-B-2. Response Matrix: Storage and Manipulation

Several schemes have been employed to facilitate efficient management of the required response data (a complete discussion of the generation and calibration of the SPI response matrices is presented elsewhere: Sturner et al 2003; Attie et al 2003; Sizun et al 2004). First, a decomposition into physically distinct matrix components is employed. This involves the different off-diagonal continuum shapes which result from partial energy-loss events within a detector volume, and events which scatter into a detector from passive material. Template forms for each case, along with a diagonal (delta function) term, comprise a basis set from which a specific direction, detector specific matrix can be reconstructed. In terms of familiar XSPEC response data types, this expressed as, e.g. $R=\Gamma_i\{arf_1^i rmf_1+arf_2^i rmf_2+arf_3 irmf_3\}$. Here the *arf*'s depend on detector and direction, while the *rmf*'s are the fixed templates as

described. Here the summation is over *p* and *d*. We note the the tools *SPIARF* and *SPIRMF* create the *arf*'s, and allow the user to resample *the rmf*'s to the desired energy binning. By implementing the linear re-combination step dynamically inside the fitting algorithm, a substantial savings in memory is achieved. In addition to the linear decomposition, the scope of the file management problem has been greatly reduced by invoking a new, SPI-sepcficic *arf-II* data structure. Here, in analogy to the multiple spectra contained in each *pha-II* structure, many individual arfs are stored in a single (3-D) fits table.

IV-B-.3. Background Solution

As noted, one must solve for the background and sources simultaneously. Unlike with differencing experiments (which alternatively point on- and off-source) or focusing instruments, there is no reliable way to simply subtract the background from the count data as an initial step. For example, in a typical Crab observation source-to-background count ration in the detector array is ~1%. Unlike sources, which are fitted by applying a photon-flux model to the appropriate instrument response, the background is modeled in count space; *i.e.* a unit response is applied to the background model for fitting. Also, the model is empirical rather than physically motivated.

To assess the accuracy of the background determination, we have compared the derived background from a Crab observation to a "blank-field" exposure obtained earlier in the mission. As can be seen (Figure IV-1), the results are reasonable. However, the significant energy dependent variability, particularly in certain instrumental line features is readily evident. Also notable is a pronounced, broad feature in the ~1.2-1.3 MeV region which is due to detector electronic effects.

IV-C: TEST RESULTS

IV-C-1 Cygnus Region

Extensive coverage of the Cygnus region was obtained during the performance verification (PV) phase of the mission in late 2002. We first attempted to model Cygnus X-1, which is of course the brightest source in that region. An example of one attempt is shown in figure IV-2. Note that the varying degrees of shadowing result in the vertical displacement of the spectral forms. The background (upper, line-dominated curve overlaid with data points), on the other hand, is nearly independent of the shadow pattern. In this case, the model fit is a cut-off power law, with spectral index α =1.8, and an exponential cut off energy of 88 keV. The derived flux agrees with that of a contemporaneous RXTE/HEXTE measurement to within a few percent, but same model extrapolated to lower energies different by ~10% from RXTE/PCA.

IV-C-.2 Crab Observations

INTEGRAL made extensive observations of the Crab region during 2003 for calibration purposes. We made use of these data to further validate the XSPEC-12 method and to compare our results to other methods. Figure IV-3 depicts the photon model fit derived for the Crab observations of revolution 0044, along with the derived background rates. Averaging over detectors (using the "setplot group" feature of XSPEC) has been used to make the information content of this type of plot manageable.

The inferred photon flux parameters (simple power-law model, using data above 35 keV) are: α =2.12 and a 1 keV flux = 11.51 ph/cm2/s/keV ie a 100 keV flux = 6.4 10-4 ph/cm2/s/keV. See section II-A and III-D for comparison with other measurements and methods.

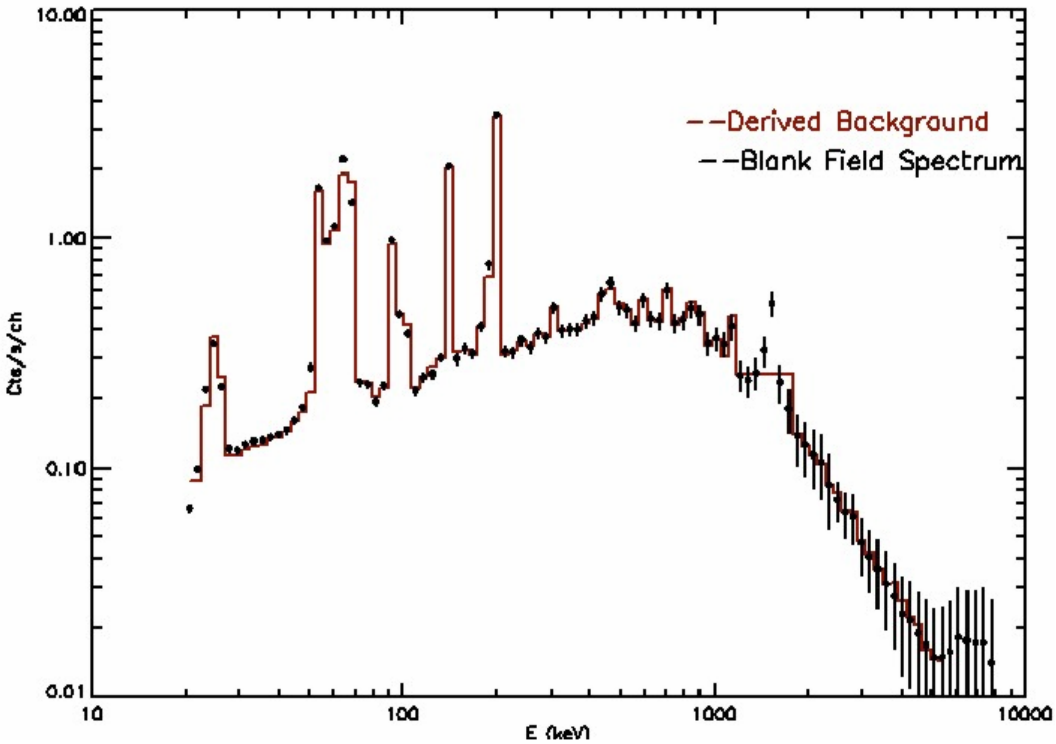

Figure IV- 1
Comparison between a typical background solution obtained from the XSPEC v12 analysis of a revolution-44 Crab observation with a “blank field” observation.

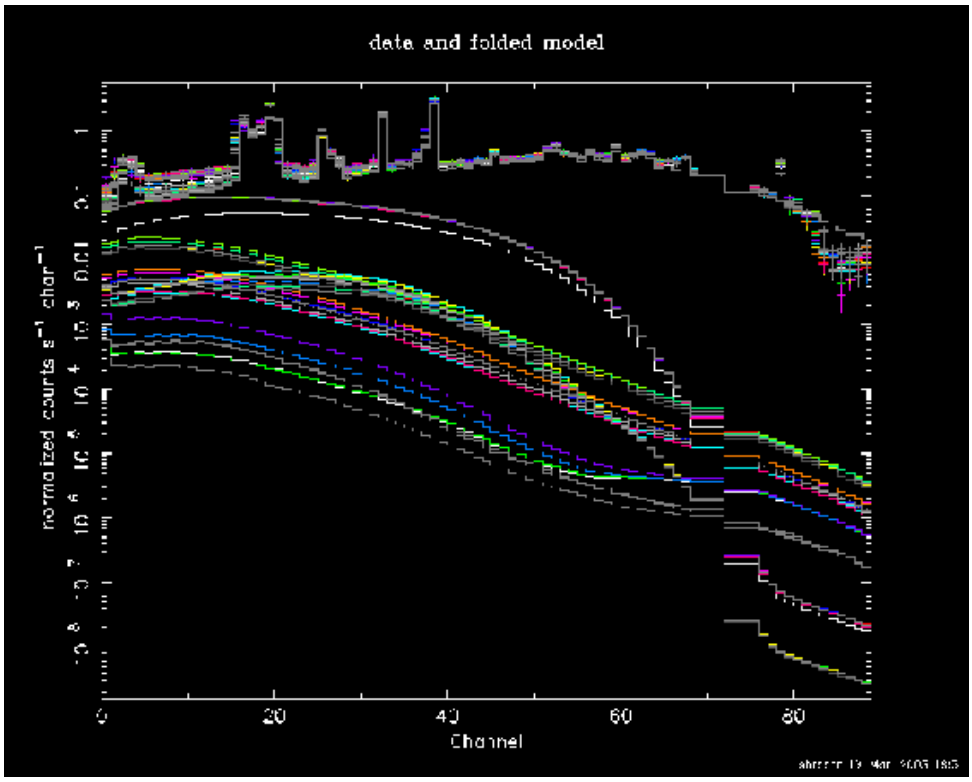

Figure IV- 2
Sample of 2-source (Cyg X-1 and Cyg X-3) plus background solution for the PV phase Cygnus region observations. Again, only a subset of the spectra are shown for purpose of clarity. The plot is in count space, with the model curves for two sources illustrating the degrees of shadowing. The upper line graphs are the background and total models, overlaid with the data.

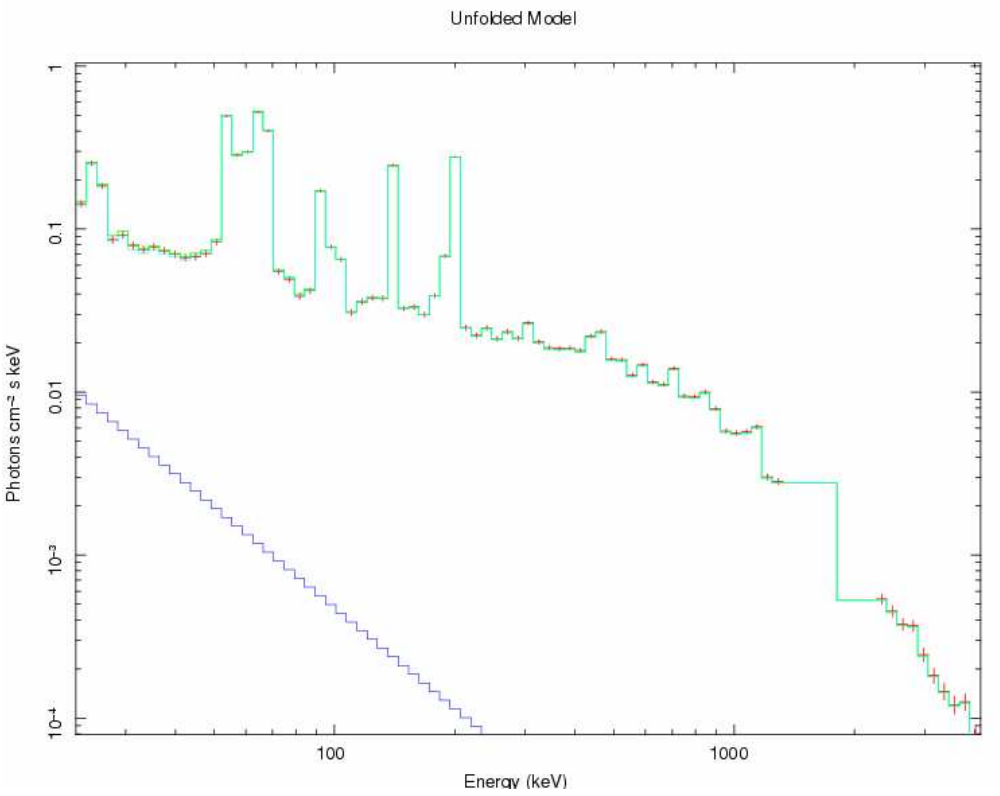

Figure IV-3
The inferred Crab spectrum plotted in photon space (model fit is the lower power-law curve). The upper curves are the total (i.e. background + source) and background model fits, overlaid by the data.

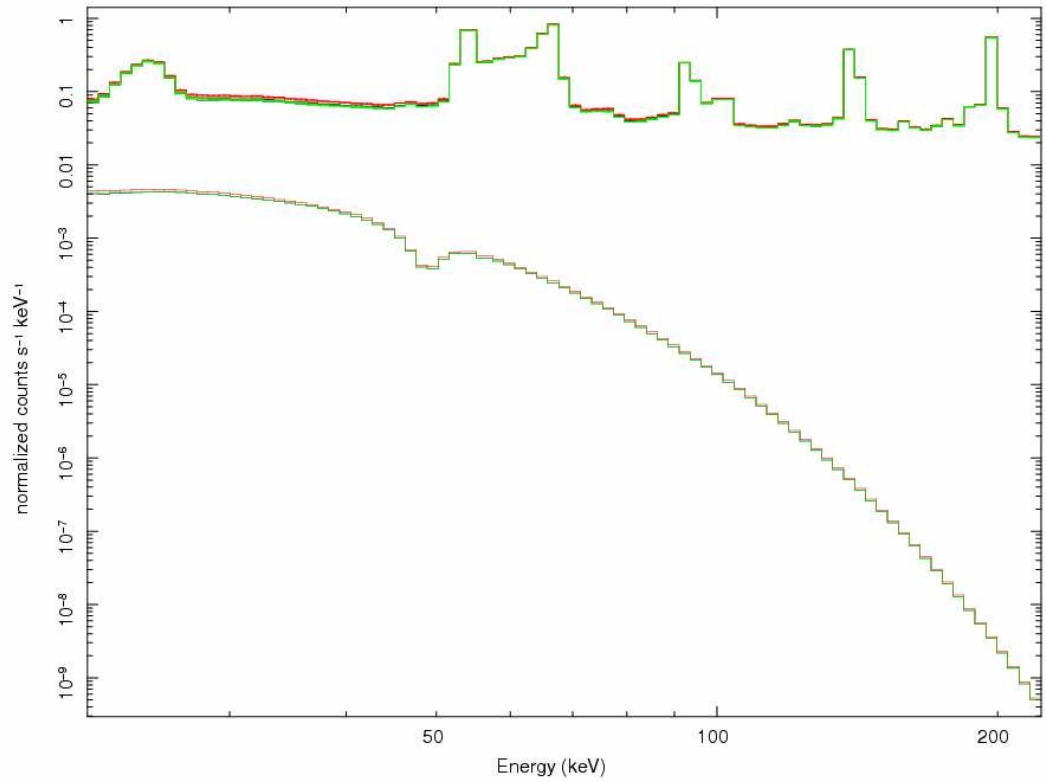

Figure IV-4
SPI spectrum of Vela X-1, revolution 82 (not discussed in the text). The continuum is modeled as an exponential times a power law, plus a cyclotron resonance feature at about 50 keV. The putative 25-keV fundamental resonance is not detected, with SPI, nor with various other instruments. In ongoing work, we are constructing spectra that are coarsely resolved in spin-phase (the spin periods is about 283 seconds), to perform a more detailed study of the cyclotron resonance profile(s).

REFERENCES

Arnaud, K., et al., 1996, A.S.P. Conf. Series, 101, G.H. Jacoby and J. Barnes, eds., p. 17.
Attie, D., et al., 2003, A&A, 411, L71
Diehl, et al., 2003, A&A, 411, L117
Dubath et al, 2005, MNRAS, 357, 401
Sizun, P., et al, 2004, proc. Fifth INTEGRAL Workshop, SP-552
Skinner, G. & Connell, P., 2003, A&A, 411, L123
Sturner, S., et al., 2003, A&A, 411, L81